

Three-Dimensional Triple-Resonance NMR of $^{13}\text{C}/^{15}\text{N}$ -Enriched Proteins Using Constant-Time Evolution

ROBERT POWERS, ANGELA M. GRONENBORN, G. MARIUS CLORE, AND AD BAX

*Laboratory of Chemical Physics, National Institute of Diabetes and Digestive and Kidney Diseases,
National Institutes of Health, Bethesda, Maryland 20892*

Received April 10, 1991

Recently it has been convincingly demonstrated that 3D triple-resonance NMR provides a practical alternative for obtaining sequential resonance assignments in larger proteins (1, 2). This approach requires a set of five or six 3D NMR experiments that correlate the various protein backbone nuclei. Details regarding the mechanisms and technical implementations of these experiments have been described previously (3–5). Two of the experiments used in this approach correlate backbone $\text{H}\alpha$ and $\text{C}\alpha$ resonances with either the intrareidue carbonyl resonance (CO) or the ^{15}N resonance of the succeeding residue and are referred to as HCACO and HCA(CO)N, respectively. The present Communication describes a modification of these experiments which optimizes their sensitivity and removes the F_1 antiphase character of correlations.

The pulse schemes of the original HCACO and HCA(CO)N experiments are very similar to the new versions that are shown in Fig. 1. The original schemes differ from the new schemes only by having a variable length evolution period of duration t_1 between the first pair of simultaneously applied 90° ($^1\text{H}/^{13}\text{C}\alpha$) pulses and the second pair of 90° pulses, applied to $^{13}\text{C}\alpha$ and ^{13}CO , instead of the fixed-time duration, $2T$. In both original schemes a 180° ^1H pulse is applied at the midpoint of t_1 to remove $\text{H}\alpha$ – $\text{C}\alpha$ J coupling (3). Before discussing the improved performance of the new schemes we briefly outline the basic principle of the original sequences.

In both original experiments, $\text{H}\alpha$ magnetization is transferred to $\text{C}\alpha$ using an INEPT scheme. At the end of the t_1 period, $\text{C}\alpha$ magnetization is transferred to the CO nucleus. In the HCACO experiment this CO magnetization evolves in the transverse plane during the second evolution period, t_2 , prior to being transferred back to $\text{C}\alpha$ and $\text{H}\alpha$ for detection. In the HCA(CO)N experiment, $\text{C}\alpha$ magnetization is also transferred to the CO nucleus, but it is subsequently relayed to ^{15}N in an HMQC manner, prior to transferring this magnetization back via CO to $\text{C}\alpha$ and $\text{H}\alpha$ for detection. Full details and an operator formalism description of the magnetization transfers involved have been given previously (3). To clarify the modification described in the present Communication, the pertinent product-operator formalism terms describing the magnetization transfers are briefly repeated for the HCACO experiment, with irrelevant constants omitted. Spin operators for $\text{H}\alpha$, $\text{C}\alpha$, and CO are denoted by I, A, and S, respectively.

At the start of the t_1 evolution period, $\text{C}\alpha$ magnetization is antiphase with respect to its attached $\text{H}\alpha$ proton and in-phase with respect to the directly attached $\text{C}\beta$ and

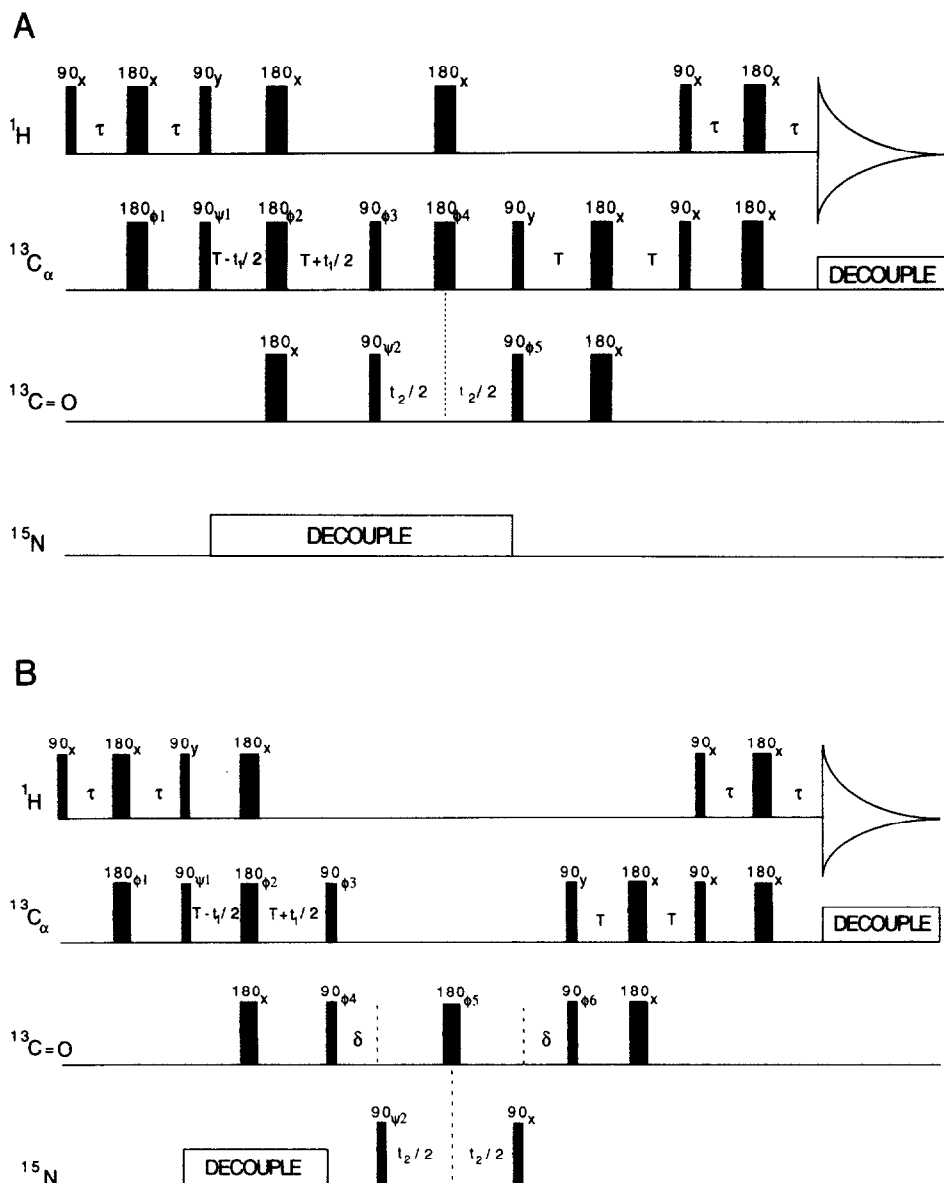


FIG. 1. Pulse schemes of (A) the CT-HCACO and (B) the CT-HCA(CO)N experiment. The phase cycling used for CT-HCACO is as follows: $\psi_1 = x$; $\psi_2 = x, -x$; $\phi_2 = 4x, 4(-x)$; $\phi_3 = 8x, 8(-x)$; $\phi_4 = 8x, 8(-x)$; $\phi_5 = 2x, 2(-x)$; Acq. = $x, 2(-x), x, -x, 2x, -x$. The phase cycling used for the CT-HCA(CO)N experiment is $\psi_1 = x$; $\psi_2 = x, -x$; $\phi_1 = 8x, 8(-x)$; $\phi_2 = 16x, 16(-x)$; $\phi_3 = 8y, 8(-y)$; $\phi_4 = 2x, 2(-x)$; $\phi_5 = \phi_6 = 4x, 4(-x)$; Acq. = $x, 2(-x), x, -x, 2x, 2(-x), 2x, -x, x, 2(-x), x$. For both schemes quadrature detection in the t_1 and t_2 dimensions is obtained by altering the phases ψ_1 and ψ_2 in a States-TPPI manner (10). The durations of the fixed delays are $\tau = 1.5$ ms; $T = 3.5$ ms; $\delta = 18$ ms.

CO nuclei. In the original scheme, this transverse magnetization dephases under influence of the $J_{C\alpha CO}$ and $J_{C\alpha C\beta}$ couplings which are active during the t_1 evolution period. Ignoring $C\alpha$ transverse relaxation, at the end of the t_1 period the fraction of magnetization that will be transferred to the CO nucleus by the subsequent $90^\circ C\alpha$ and CO has evolved according to

$$A_y I_z \xrightarrow{t_1} A_x I_z S_z \sin(\pi J_{C\alpha CO} t_1) \cos(\pi J_{C\alpha C\beta} t_1) \cos(\Omega_A t_1), \quad [1]$$

where Ω_A is the angular offset frequency of $C\alpha$. Because the phase cycling of the experiment selects the magnetization-transfer pathway described by expression [1], the signal observed during t_3 is modulated in intensity by $\sin(\pi J_{C\alpha CO} t_1) \cos(\pi J_{C\alpha C\beta} t_1) \cos(\Omega_A t_1)$. Fourier transformation in the t_1 domain therefore results in a multiplet centered at $F_1 = \Omega_A/2\pi$, with an antiphase $J_{C\alpha CO}$ (~ 55 Hz) splitting and an in-phase $J_{C\alpha C\beta}$ (~ 35 Hz) splitting. To maximize the magnetization transfer, and thus the sensitivity of the experiment, it is important to maximize the average value of $\sin(\pi J_{C\alpha CO} t_1) \cos(\pi J_{C\alpha C\beta} t_1)$. Previously, this was done by restricting the acquisition period in the t_1 dimension to a value significantly shorter than $\sim 1/(2J_{C\alpha C\beta})$, about 11 ms in practice, causing the passive $J_{C\alpha C\beta}$ splitting to remain unresolved. The $\sin(\pi J_{C\alpha CO} t_1)$ term in expression [1] gives rise to an antiphase $J_{C\alpha CO}$ splitting in the F_1 dimension of the resulting 3D spectrum, causing some problems during automated peak picking, especially for (partially) overlapping resonances.

Here we show that constant-time versions (6–8) of the HCACO and HCA(CO)N experiments can be successfully used to eliminate all J splittings from the F_1 dimension. This also permits optimization of the magnetization transfer, independent of the t_1 duration. The modified constant-time versions of the HCACO and HCA(CO)N experiments, named CT-HCACO and CT-HCA(CO)N, are shown in Fig. 1. The total duration of the constant-time period during which transverse $C\alpha$ magnetization is present is $2T$. Three 180° pulses are applied simultaneously to 1H , $^{13}C\alpha$, and ^{13}CO during this period at a time $T - t_1/2$ after the first $90^\circ C\alpha$ pulse. The magnetization-transfer expression of Eq. [1] is now transformed into

$$A_y I_z \xrightarrow{2T, t_1} A_x I_z S_z \sin(2\pi J_{C\alpha CO} T) \cos(2\pi J_{C\alpha C\beta} T) \cos(2\pi J_{H\alpha C\alpha} T) \cos(\Omega_A t_1). \quad [2]$$

Again, the effect of $C\alpha T_2$ has been ignored in expression [2]. Magnetization transfer and thus sensitivity is maximized when the product at the right-hand side of expression [2] is maximized.

Resolution in the t_1 dimension is limited by the fact that the t_1 acquisition period is restricted to the constant-time duration, $2T$. As a reasonable compromise between high sensitivity and acceptable resolution, we use a constant-time duration, $2T$, equal to 7 ms. Because the duration of 7 ms also corresponds to $\sim 1/J_{H\alpha C\alpha}$, the $C\alpha$ spin will be antiphase with respect to the $H\alpha$ proton at the end of the time $2T$, as was the case in the regular HCACO experiment.

In the constant-time experiments there is no decay in the t_1 dimension caused by T_2 relaxation nor is there any t_1 dependence of dephasing caused by J couplings (6). Thus, a typical data set obtained for a protein shows modulation in the t_1 dimension by a limited number of nondecaying cosines. As is discussed later, this type of truncated

time-domain signal can be extended profitably by “mirror-image” linear prediction (9).

The constant-time 3D experiments have been used for backbone resonance assignment of the ribonuclease H (RNase H) domain of HIV reverse transcriptase. The RNase H domain consists of 138 residues and has a molecular weight of 15.2 kDa. The sample concentration was 1.1 mM, pH 5.4, and spectra were recorded at 25°C on a Bruker AM-600 spectrometer, modified as described previously (3). The acquired data matrices comprised 32 complex data points in the t_1 ($C\alpha$) dimension and 512 real points in the t_3 ($H\alpha$) dimension for both the CT-HCACO and CT-HCA(CO)N experiments. For the CT-HCACO experiment, 64 complex data were sampled in the t_2 (CO) dimension and for the HCA(CO)N experiment, 32 complex data were sampled in the t_2 (^{15}N) dimension. Spectral widths were 15.13, 29.16, 33.13, and 8.33 ppm in the ^{13}CO , ^{15}N , $^{13}\text{C}\alpha$, and ^1H dimensions, respectively. In the RNase H domain a number of the ^1H , ^{13}C , and ^{15}N resonances have linewidths substantially larger than those observed for the majority of the resonances. Because for residues with these broadened resonances the J connectivities observed in the 3D experiments are weak, relatively long accumulation times were necessary for both 3D experiments (~ 3 days per 3D spectrum) to maximize the number of observable connectivities.

As mentioned above, signal in the constant-time dimension (t_1 , $C\alpha$) does not decay and it is therefore ideally suited for extension in this dimension by means of the mirror-image linear prediction technique. Because the phase of the signals is zero at $t_1 = 0$, data at negative times (not acquired) are the complex conjugates of the acquired data at positive t_1 values. These “negative-time” data are added to the t_1 time domain and this artificially lengthened time domain is then used as input for a linear prediction algorithm that lengthens the time domain by 50% in the positive-time direction. After discarding the negative-time data, the extended t_1 time domain thus comprises 64 complex data points, resulting in acceptable resolution in the $C\alpha$ dimension, despite the relatively short acquisition time (6.4 ms) used in the corresponding time domain (t_1).

Zero filling was used in all three dimensions and the absorptive part of the final 3D spectrum consisted of $128 \times 128 \times 512$ data points for both 3D spectra. Shifted sine-bell filtering was used in all three dimensions for both spectra.

Figure 2A shows a typical (F_1 , F_2) slice taken through one of the most crowded regions of the CT-HCACO spectrum, displaying correlations between $C\alpha$ and CO for residues with an $H\alpha$ shift in the vicinity of 4.30 ppm. Similarly, Fig. 2B is an (F_1 , F_2) slice taken from the CT-HCA(CO)N spectrum at an F_3 shift of 4.30 ppm, showing the corresponding correlations between $C\alpha$ and the ^{15}N resonance of the next residue. For both spectra all resonances are purely absorptive in all three orthogonal frequency dimensions, providing optimal resolution and minimal distortion in the limited number of cases where spectral overlap occurs.

In the original HCACO and HCA(CO)N experiments the duration of the t_1 evolution period is systematically incremented and the transfer of magnetization from $C\alpha$ to carbonyl has a sinusoidal dependence on t_1 (3), with a maximum near $t_1 = 7$ ms. The constant-time versions of the triple-resonance experiments described here provide a significant enhancement in sensitivity by keeping the $C\alpha$ to carbonyl magnetization-transfer optimized at the constant-time duration, $2T = 7$ ms. In addition,

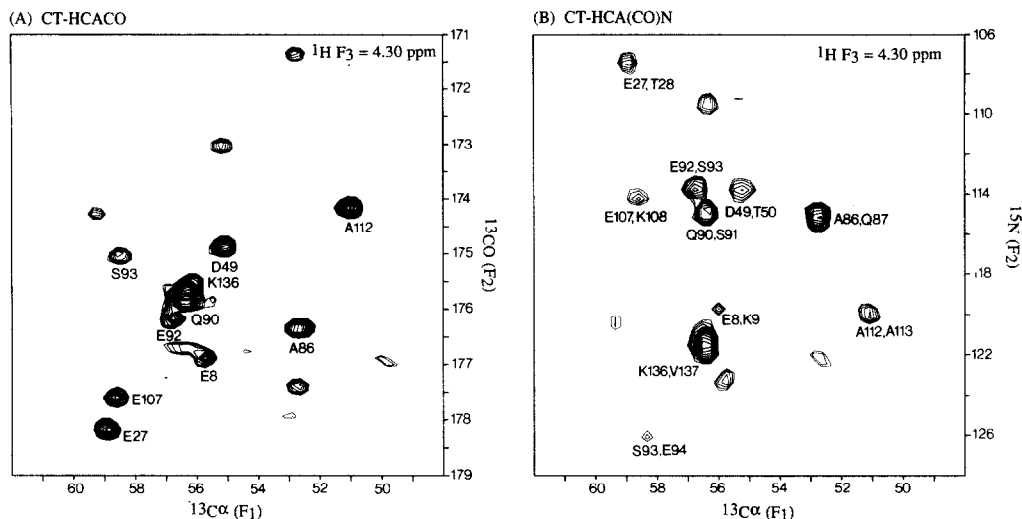


FIG. 2. Sections of (F_1 , F_2) slices taken from the (A) CT-HCACO and (B) CT-HCA(CO)N spectra of the RNase H domain of reverse transcriptase. Both slices are taken perpendicular to the F_3 axis, at a ^1H chemical shift of 4.30 ppm. The t_1 time domain has been extended twofold (up to 14 ms) by mirror-image linear prediction. The CT-HCACO spectrum shows intrasidue correlations between C_α and H_α for residues with an H_α shift near 4.30 ppm. The CT-HCA(CO)N spectrum shows interresidue connectivity between the C_α of a residue that has its H_α resonance near 4.30 ppm and the ^{15}N resonance of the succeeding residue.

since the $J_{C_\alpha\text{CO}}$ coupling is eliminated from the spectrum, resonances in the F_1 dimension have an absorptive singlet shape instead of the antiphase doublet shape observed in the original experiments, making it easier to perform automated peak picking.

ACKNOWLEDGMENTS

We thank Lewis Kay and Mitsuhiro Ikura for useful discussions, Guang Zhu and Lewis Kay for developing the mirror image linear prediction software, and Rolf Tschudin for continuous expert technical assistance. This work was supported by the Intramural AIDS Directed Antiviral Program of the Office of the Director of the National Institutes of Health.

REFERENCES

1. M. IKURA, L. E. KAY, AND A. BAX, *Biochemistry* **29**, 4659 (1990).
2. M. IKURA, L. E. KAY, M. KRINKS, AND A. BAX, *Biochemistry*, in press.
3. L. E. KAY, M. IKURA, R. TSCHUDIN, AND A. BAX, *J. Magn. Reson.* **89**, 496 (1990).
4. L. E. KAY, M. IKURA, AND A. BAX, *J. Magn. Reson.* **91**, 84 (1991).
5. A. BAX AND M. IKURA, *J. Biomol. NMR*, in press.
6. A. BAX, A. F. MEHLKOPF, AND J. SMIDT, *J. Magn. Reson.* **35**, 373 (1979).
7. A. BAX AND R. FREEMAN, *J. Magn. Reson.* **44**, 542 (1981).
8. O. W. SØRENSEN, *J. Magn. Reson.* **90**, 433 (1990).
9. G. ZHU AND A. BAX, *J. Magn. Reson.* **90**, 405 (1990).
10. D. MARION, M. IKURA, R. TSCHUDIN, AND A. BAX, *J. Magn. Reson.* **85**, 393 (1989).